Effects of emodin on intestinal mucosal barrier by the upregulation of miR-218a-5p expression in rats with acute necrotizing pancreatitis

Yang Tan*, Wei Zhang*, Hai-ying Wu, Jing Xia, Huang-bo Zhang, Ming-wei Liu (iD) **and Chuan-yun Qian** (iD)

Abstract

Emodin is an effective component in rhubarb to cure intestinal dysfunction, but the specific mechanism remains unknown. This study aimed to evaluate the protective effects of emodin on intestinal dysfunction caused by acute severe pancreatitis and reveal the functional mechanism of emodin in the treatment of this condition. An acute severe pancreatitis model was prepared using taurocholate. In the treatment group, 50 mg/kg emodin was injected intravenously 2 h before the induction of acute severe pancreatitis at an interval of 8 h. After 24 h, the gene expression and protein levels of miR-218a-5p, RhoA, ROCK1, Akt, Notch1, Bax, Bcl-2, Fas, FasL, caspase-3, and caspase-9 were determined through reverse transcription polymerase chain reaction and Western blot analysis. The protein levels of occludin, zonula occludens-1 (ZO-1), and E-cadherin in the intestinal tract were also determined through Western blot analysis. The effects of miR-218a-5p on the apoptosis of rat intestinal epithelial cell-18 were observed through flow cytometry. The effects of emodin on intestinal cell apoptosis induced by acute severe pancreatitis were observed via TUNEL (terminal deoxynucleotidyl transferase dUTP nick-end labeling). Pathological changes in the pancreas and intestine of rats in each group were observed through hematoxylin and eosin staining. After 24 h of acute severe pancreatitis induced by taurocholate, emodin reduced the expression of miR-218a-5p in the intestinal tract; increased the expression of Notch1 and Bcl-2; decreased the expression levels of RhoA, ROCK1, Akt, Bax, Fas, FasL, caspase-3, and caspase-9; inhibited the intestinal cell apoptosis caused by acute severe pancreatitis; increased the protein expression levels of occludin, zonula occludens-1 (ZO-1), and E-cadherin in the intestinal tract; and alleviated intestinal dysfunction caused by acute severe pancreatitis. Emodin could regulate Notch1 and RhoA/ROCK pathways by regulating the miR-218a-5p expression in the intestine. It could also inhibit intestinal cell apoptosis induced by acute severe pancreatitis and improve the intestinal dysfunction caused by severe acute pancreatitis.

Keywords

acute pancreatitis, emodin, intestinal mucosal barrier, miR-218-5p, Notch1, RhoA/ROCK

Introduction

Severe acute pancreatitis (SAP) is an acute abdominal disease that has a rapid onset and is dangerous; its mortality rate can be as high as 20%–40%.[1] SAP may be related to the mechanisms of self-digestion of the pancreas, the cascade of inflammatory mediators caused by pancreatic tissue damage, pancreatic blood circulation disorder induced by inflammatory mediators and vasoactive substances, and secondary infection of the pancreas due to

Department of Emergency, First Affiliated Hospital of Kunming Medical University, Kunming, China

*These authors contributed equally to this work.

Corresponding authors:
Ming-wei Liu, Department of Emergency, First Affiliated Hospital of Kunming Medical University, 295 Xichang Road, Wu Hua District, Kunming 650032, China.
Email: lmw2004210@163.com

Chuan-yun Qian, Department of Emergency, First Affiliated Hospital of Kunming Medical University, 295 Xichang Road, Wu Hua District, Kunming 650032, China.
Email: lmw2004210@tom.com

intestinal bacterial translocation; however, its pathogenesis has yet to be fully studied.[1–4] Studies have found that the leading causes of death are secondary bacterial infections after pancreatic tissue necrosis in SAP, subsequent systemic inflammatory response syndrome, and multiple organ failure.[2–4] Related experimental studies have confirmed that the bacterial infection of SAP is caused by intestinal bacterial translocation attributed to the SAP-induced destruction of the intestinal mucosal barrier.[5] Therefore, enhancing the regeneration of the intestinal mucosal epithelium and repair, maintaining the integrity of the intestinal mucosal barrier, enhancing the intestinal immune function, and reducing the release of inflammatory mediators and cytokines[4,5] can improve the prognosis of patients with SAP.

Emodin (1,3,8-trihydroxy-6-methyl-anthraquinone) is the main active ingredient of the Chinese medicine rhubarb. Modern pharmacological research has revealed that emodin has various functions, including antioxidation, free radical scavenging, anti-inflammatory, anti-tumor, and anti-apoptosis.[6–8] Rhubarb is used to treat SAP, improve intestinal mucosal dysfunction caused by SAP, and significantly reduce the mortality of patients with SAP.[7,8] However, the underlying mechanism remains unclear and needs further studies.

MicroRNAs (miRNAs), a class of small noncoding RNAs, are widely found in the nucleus of plants and animals. Their mature precursors usually have approximately 18–22 bp. miRNAs can degrade messenger RNA (mRNA) or silence translation mainly by entirely or partially binding to the 3′-untranslated region (UTR) of target mRNA genes, thereby regulating gene expression.[9] Studies on pulmonary fibrosis have shown that miRNAs are involved in many key processes, such as inflammation, proliferation, autophagy, apoptosis, and fibrosis, by regulating different signaling pathways.[9–11] The apoptosis of human umbilical vein endothelial cells can be promoted by the downregulation of miR-218-5p that induces the high mobility of group protein-1 in allergic purpura.[12]

The RhoA/ROCK signaling pathway can help maintain the balance of the number of epithelial cells and the renewal rate of epithelial tissues by participating in the regulation of the apoptosis of intestinal epithelial cells.[13] In pathological states such as inflammation, ROCK can accelerate the apoptosis rate of epithelial cells by various mechanisms, affect the intercellular junction structure and ligand, inhibit cell differentiation, weaken the integrity of the intestinal barrier, cause local inflammation to spread throughout the body, and aggravate disease development.[13] The NOTCH signaling pathway achieves intracellular signaling and transcription through local cell-to-cell interactions, thereby controlling cell proliferation, differentiation, autophagy, apoptosis, migration, and adhesion.[12]

Apoptosis plays important roles in intestinal mucosal damage caused by SAP. In this experiment, we hypothesized that miR-218-5p might participate in SAP-induced intestinal mucosal injury by regulating intestinal cell apoptosis to examine the protective mechanism of emodin on intestinal mucosal injury induced by SAP. This study also aimed to determine whether emodin could ameliorate the intestinal mucosal barrier dysfunction caused by SAP by blocking the RhoA/ROCK and NOTCH apoptosis pathway through the regulation of the miR-218-5p expression. This study provided a new theoretical basis and therapeutic target for administering emodin to treat SAP-induced intestinal mucosal dysfunction.

Materials and methods

Cell culture

Rat intestinal epithelial cell-6 (IEC-6; ATCC, Manassas, VA, USA) was cultured in a 1640 medium in an incubator with 5% CO_2 and constant humidity at 37°C. After the cells grew by more than 95%, they were washed with phosphate-buffered saline (PBS), trypsinized, and observed under a microscope. The medium was added to terminate digestion when the cells appeared to be rounded. These cells were divided into three flasks and subcultured. When they grew well, those in the logarithmic growth phase were used for subsequent experiments.

miRNA mimics, inhibitor, and gene transfection

IEC-6 cells were cultured in 6-well plates until 40% confluence was reached. miR-218-5p mimics, miR-218-5p mimic-negative control (NC), miR-218-5p inhibitor, and miR-218-5p inhibitor-NC were mixed with Lipofectamine 2000 (Invitrogen, NY, USA) and added to the cell culture medium in accordance

with the manufacturer's instructions. After 24 h of transfection, total RNA and protein were prepared from the cells and subjected to quantitative reverse transcription polymerase chain reaction (qRT-PCR) and Western blot analyses, respectively.

miR-218-5p target gene prediction and dual-luciferase reporter assay

TargetScan (http://www.targetscan.org), PicTar (www.pictar.org), and miRBase (www.mirbase.org) were used to predict candidate miR-218-5p targets. IEC-6 cells (1×10^5) were cultured in 24-well plates and then transfected with Rock1-3′ UTR-wild-type (wt) or Rock1-3′-UTR-mutant (mt), and miR-218-5p or miR-218-5p-NC with Lipofectamine 2000 (Invitrogen). Luciferase activity was measured 24 h after transfection with a Dual-Luciferase Reporter Assay System (Promega, Madison, WI, USA). The results were normalized to *Renilla* activity.

Animals

One hundred twenty male Sprague-Dawley rats (Kunming Medical University Laboratory Animal Center, Kunming, China) were housed in the Kunming Medical University Animal Care Facility and maintained under pathogen-free conditions. The environment was maintained at a relative humidity of 30%–70%. The rats were 8–9 weeks old at the initiation of the experiments and maintained on standard laboratory chow and water ad libitum. All the experiments were approved and conducted in accordance with the guidelines of the Animal Care Committee of Kunming Medical University. The experimental procedures were approved by the ethics committee of the Institute of the Kunming Medical University (Approval Number: KYYM-2018-012-C11) and performed in accordance with institutional guidelines and ethics. This study was also compliant with international, national, and institutional guidelines for humane animal treatment and relevant legislation.

Taurocholate-induced pancreatitis

The rats were anesthetized by intraperitoneally injecting 1% pentobarbital sodium (35 mg/kg body weight), and the operation was performed under aseptic conditions. SAP models were prepared in accordance with the method proposed by Liu et al.[14] and Aho et al.[15] Sham-operated (SO) animals were subjected to the same surgical procedures, but *taurocholate* was not actively infused into the pancreas.

Tail intravenous administration of AdCMV-miR-218-5p

A constitutively active miR-218-5p expression construct was delivered to the rats via the tail intravenous administration of 1×10^9 pfu of AdCMV-miR-218-5p after 14 days in accordance with previously described methods[14] to construct miR-218-5p-expressing rats. A taurocholate-induced pancreatitis model group (model group; n = 10) and an SO group (n = 10) were prepared, and miR-218-5p-expressing rats were used to induce miR-218-5p model rats (n = 10) and miR-218-5p SO rats (n = 10). After the rats were subjected to taurocholate-induced acute pancreatitis and intestinal damage for 24 h, they were anesthetized with intravenous pentobarbital sodium (50 mg/kg) and sacrificed via cervical dislocation. Their intestinal tissues were obtained, used for real-time PCR and Western blot analysis, and stained with hematoxylin and eosin (H&E) to observe pathological changes in intestinal tissues.

Animal groups and treatments

According to a random number table, 80 rats were randomly divided into four groups: SO group (n = 20), emodin-treated SO group (SO treatment group; n = 20), SAP model group (model group; n = 20), and emodin treatment model group (model treatment group; n = 20). As previously described,[7] the SO treatment group and the model treatment group were intraperitoneally injected with emodin (50 mg/kg) 2 h before pancreatitis was induced by taurocholate. Injection was administered once every 8 h. The SO and model groups were given the same volume of saline. After the animals in each group were anesthetized with 1% pentobarbital sodium (50 mg/kg body weight; Wuhan Dinghui Chemical Co., Ltd., Wuhan, China) and euthanized through cervical dislocation at 24 h, the right internal carotid artery was isolated. Blood was extracted (5 mL), centrifuged to collect the supernatant, dispensed into two sterile tubes, sealed with sealing glue, and placed in a freezer at −20°C until use.

Table 1. Primer sequences of genes for the RT-PCR analysis.

miR-218-5p	F-5′-GGTAATGACACGATCACTCC-3′	215 bp
	R-5′-CAGTGCGTGTCGTGGAG-3′	
U6	F-5′GTGCTCGCTTCGGCAGCACATATAC-3′	237 bp
	R-5′-AAAAATATGGAACGCTCACGAATTTG-3′	
Rho mRNA	F-5′-ACGGGAAGCAGGTAGAGTTG-3′	198 bp
	R-5′-CTAGGATGATGGGCACATTTGG-3′	
Akt mRNA	F-5′-TCACCTCTGAGACCGACACC-3′	174 bp
	R-5′-ACTGGCTGAGTAGGAGAACTGG-3′	
Notch1 mRNA	F-5′-TGGGTGGACAAGATCAACG-3′	171 bp
	R-5′-GGTCCCCGTGTAACCTTCTG-3′	
Rock1 mRNA	F-5′-GACCTACTGCTGTGTTGGAATC-3′	187 bp
	R-5′-TAGGCAAACCCGCAAGAAAC-3′□□	
Fas	F-5′-GACCCAGAATACCAAGTGCAAGTG-3′	184 bp
	R-5′-CTTGCCCTCCTTGATGTTATTTTC-3′	
FasL	F-5′-CGTGAGTTCACCAACCAAAGC-3′	163 bp
	R-5′-CCCAGTTTCGTTGATCACAAG-3′	
Caspase-3	F-5′-CATGGAAGCAAGTCGATGGA-3′	114 bp
	R-5′-CGGCAGTAGTCGCCTCTGA-3′	
Bcl-2	F-5′-ATGTGTGTGGAGAGCGTCAA-3′	98 bp
	R-5′-GAGACAGCCAGGAGAAATCAA-3′	
Bax	F-5′-ACCAAGAACCTGACCGGAGTGTC-3′	265 bP
	R-5′-ACAAAGATGGTCACCGGTCTGGCC	
β-actin	F-5′-GATTACTGCTCTGGCTCCTGC-3′	190 bp
	R-5′-GACTCATCGTACTCCTGCTTGC-3′	

RT-PCR: reverse transcription polymerase chain reaction; mRNA: messenger RNA.

Serum and ascites were obtained to measure amylase levels and ascitic capacity. Pancreatic and small intestinal tissues were quickly removed and fixed in 10% formalin for morphological studies. Portions of the pancreatic and small intestinal tissues were freshly processed to determine pancreatic water contents.

RT-PCR analysis

IEC-6 cells or grounded intestinal tissues were soaked in RNA extraction buffer and homogenized rapidly. The total RNA of cells was extracted by Trizol, and the RNA concentration was measured using a nucleic acid quantification device. Complementary DNA (cDNA) was synthesized using a reverse transcription kit under the following conditions: reaction at 37°C for 15 min, reaction at 85°C for 5 s, and termination reaction at 4°C. PCR amplification was performed using a CFX96 Touch fluorescent quantitative PCR analyzer with β-actin as the internal reference gene of mRNA and U6 as the internal reference gene of miR-218-5p. The primer sequences are shown in Table 1. The PCR reaction system was composed of 5.0 μL of 5× SYBR Green fluorescent dye, 3.4 μL of diethylpyrocarbonate (DEPC) water, 0.2 μL of upstream and downstream primers, 1.0 μL of cDNA sample, and 0.2 μL of ROX. PCR was conducted under the following conditions: 95°C for 5 min; 95°C for 30 s, 60°C for 30 s, and 72°C for 30 s for 40 cycles. The relative mRNA expression levels of miR-218-5p, Bax, Fas, caspase-3, Bcl-2, Rock1, and Notch1 were calculated with the $2^{-\Delta\Delta Ct}$ method. The experiment was independently repeated three times.

Western blot analysis

The collected IEC-6 cells or the grounded intestinal tissues were fully lysed. The supernatant was aspirated, and 5× loading buffer was added to the supernatant, mixed, and boiled for 5 min. Afterward, 100 g/L polyacrylamide gel electrophoresis (PAGE) separation gel and 50 g/L PAGE concentration gel were prepared, and 40 μg of protein sample was added to each well. The voltage was adjusted as follows: the voltage for running the concentration gel was 80 V, and the voltage for running the separation gel was 110 V. Observation with bromophenol blue was performed. When it reached the bottom of the

separation gel, electrophoresis was terminated. The gel was taken out, and the protein on the gel was transferred to the nitrocellulose filter membrane on ice at a current of 300 mA. Afterward, 5 g of skimmed milk powder was weighed into 100 mL of TBST (Tris-Buffered Saline and Tween 20) to prepare a blocking solution. After the cells were incubated in the blocking solution for 1 h, the nitrocellulose filter membrane was, respectively, incubated in the buffer containing anti-Bax, anti-Fas, anti-caspase-3, anti-Bcl-2, anti-Rock1, and anti-Notch1 antibodies for 2 h. The NC membrane was incubated with a secondary goat anti-rabbit IgG-horseradish peroxidase (HRP) antibody (1:2000) or goat anti-mouse IgG-HRP antibody (1:2000; Santa Cruz Biotechnology, Santa Cruz, CA, USA) reaction buffer for 2 h. The enhanced chemiluminescence (ECL) solution was added to the NC membrane, and the gray value of the exposed band was scanned with Quantity One. The internal reference was β-actin. The relative expression of the target protein was equivalent to the gray value of the target protein band/gray value of the β-actin band. The experiment was independently repeated three times.

Immunohistochemical analysis

Immunohistochemical staining was conducted in strict accordance with the instructions of the SABC kit. Tissue wax was cut into slices with a thickness of about 3 μm. Dewaxing with PBS solution, dehydrating with gradient ethanol for 15 min each time, incubating with fresh 3% H_2O_2 methanol at room temperature for 30 min, and again washing with PBS solution for 3–5 min. Microwave was applied to repair Bax and caspase-3 polyclonal antibody. Endogenous peroxidase was blocked with 5% bovine serum albumin (BSA), dripped with rabbit anti-mouse Bax and caspase-3 polyclonal antibody (primary antibody working solution; BD Pharmingen, San Jose, CA, USA), incubated overnight at 4°C, rinsed with PBS for 3 × 5 min, dripped with biotin-labeled secondary antibody working solution (R&D Systems, Inc. MN, USA), and incubated for 30 min at 37°C. Streptomycin-ovalbumin working solution labeled with HRP was added and incubated for 30 min at 37 °C. Slices were removed from the incubator and added with a DAB developer (Vector Laboratories, Inc., Burlingame, CA, USA) for 10 min, rinsed with distilled water,

re-stained with hematoxylin, differentiated with hydrochloric alcohol, stained with eosin, dehydrated with gradient ethanol, cleared with xylene I and II, and sealed with neutral gum. Five slices were selected from each group of small intestinal tissue slices, and 10 non-overlapping high-power fields were randomly selected for each slice. The results showed that brown-yellow granules were positive immune complexes in the cytoplasm and/or nucleus. The granules were observed under an optical microscope (×400), photographed, and preserved. The average absorbances of Bax and caspase-3 were measured by analyzing with Image-ProPlus (IPP) 6.0 (Media Cybernetics, Inc., Rockville, MD, USA) and expressed as a positive unit (pu). Background values were also determined simultaneously.

In situ hybridization

A 5′-digoxigenin-labeled oligonucleotide probe was designed to hybridize with miR-218-5p in situ using an miRNA in situ hybridization (ISH) buffer and control kit and to observe the miR-218-5p expression in intestinal tissues (Exiqon, Woburn, MA, USA).

Detection of apoptosis using TUNEL after SAP-induced intestinal injury

As previously described,[13] digoxigenin-11-dUTP was labeled with 3′-OH formed after DNA breakage by terminal deoxynucleotidyl transferase (TdT). Peroxidase was labeled to the DNA breakpoint, and substrates were added. The apoptotic cells could be stained with a 5-bromo-4-chloro-3-indolyl-phosphate/tetrazolium blue (BCIP/NBT) (3,3'-diaminobenzidine (DAB)) staining agent. The results indicated that the gene labeled with biotin was brown yellow, so the brown-yellow granules were positive cells in the nucleus. Ten complete and non-overlapping microscopic fields (×400) were randomly selected for each slide. MoticMed 6.0, a pathological image analysis system, was used to count the percentage of positive cells and calculate the apoptotic rate.

Flow cytometric detection of the apoptotic rate of the small intestine

After 48 h of transfection, the cells were washed with pre-cooled PBS and suspended with 300 L of

buffer solution. The cell concentration was adjusted to 1×10^6/mL, and 100 µL was placed in a flow tube. Then, 5 µL of ANNEXIN V-FITC (BD Pharmingen, San Diego, CA, USA) and 5 µL of propidium iodide (PI; Abcam, Cambridge, MA, USA) were added to the tube, incubated at room temperature for 15 min, and added with 400 µL of PBS to detect cell apoptosis through flow cytometry. Apoptotic cells were quantified as the percentage of cells stained with Annexin V. The experiment was repeated three times.

Intestinal permeability

Vascular permeability was evaluated on the basis of the amount of Evans blue that penetrated the tissue.[16,17] Evans blue (20 mg/kg) was injected through the thigh veins (1 mL/kg) 2 min before reperfusion. After reperfusion, a 5-cm ileocecal part of the intestinal canal of more than 10 cm was taken out, cut open, dried at 37°C for 24 h, weighed, and extracted with Evans blue by soaking into 3 mL of formamide at room temperature for 24 h. A standard curve of Evans blue was drawn at 620 nm, and the absorbance in the extract was read to calculate the amount of Evans blue in the tissue. The result was expressed as 1 µg of Evans blue/1 g of dry weight tissue.

Histological analysis of intestinal injury after SAP-induced intestinal injury

For histological preparations, the pancreatic and small intestinal (jejunum and ileum) tissues collected from the rats were washed with ice-cold PBS and fixed overnight in 10% formalin. The tissues were subjected to automated dehydration through a graded alcohol series, embedded in paraffin, sectioned at 5 µm, and stained with H&E. Intestinal H&E sections were graded for intestinal SAP-induced mucosal injury using the Chiu score.[18] Edema, hemorrhage, and necrosis of the pancreas were graded into four levels (0 to 3) in accordance with previously described methods.[19] All H&E sections were evaluated by a pathologist (V.D.D.) blinded to the samples.

Statistical analysis

Data were analyzed with SPSS 19. 0, and measurement data were expressed as mean ± standard deviation as specified in the figure legends. Statistical comparisons between the model and treatment or SO groups were evaluated using a t-test. One-way analysis of variance (ANOVA) followed by a Student–Newman–Keuls test was conducted to compare the differences among multiple groups. Data with $P < 0.05$ were considered statistically significant.

Results

Effect of miR-218-5p on the protein expression of Bax, Fas, caspase-3, Bcl-2, Rock1, and Notch1 and the apoptosis of rat intestinal epithelial cells

miR-218-5p mimics, miR-218-5p mimic-NC, miR-218-5p inhibitor, and miR-218-5p inhibitor-NC were initially mixed with Lipofectamine 2000 (Invitrogen) to investigate the effect of miR-218-5p on the protein expression of Bax, Fas, Bcl-2, caspase-3, Rock1, and Notch1 in rat intestinal epithelial cells and subsequently added to the cell culture. After 24 h of transfection, the expression levels of Bax, Fas, Bcl-2, caspase-3, Rock1, and Notch1 were measured through Western blot. The apoptosis rate of intestinal epithelial cells was measured through flow cytometry. In Figure 1, the increase in the expression level of miR-218-5p caused a significant decrease in the protein expression levels of Bax, caspase-3, Fas, Rock1, and Notch1; an increase in the Bcl-2 expression (Figure 1(a) and (b)); and a reduction in the apoptosis rate of rat intestinal epithelial cells (Figure 1(c) and (d)). These findings suggested that miR-218-5p might play a role in regulating apoptosis signaling pathways.

Effect of miR-218-5p overexpression on rat intestinal damage after taurocholate-induced acute pancreatitis

miR-218-5p-overexpressing rats were constructed through the tail intravenous administration of 1×10^9 pfu of AdCMV-miR-218-5p after 10 days to analyze the overexpression of miR-218-5p on rats with taurocholate-induced acute pancreatitis and intestinal damage. The rats were treated with taurocholate through intraperitoneal injection. In Figure 2, after the rats were administered with 1×10^9 pfu of AdCMV-miR-218-5p, the expression level of miR-218-5p in the small intestinal tissues significantly
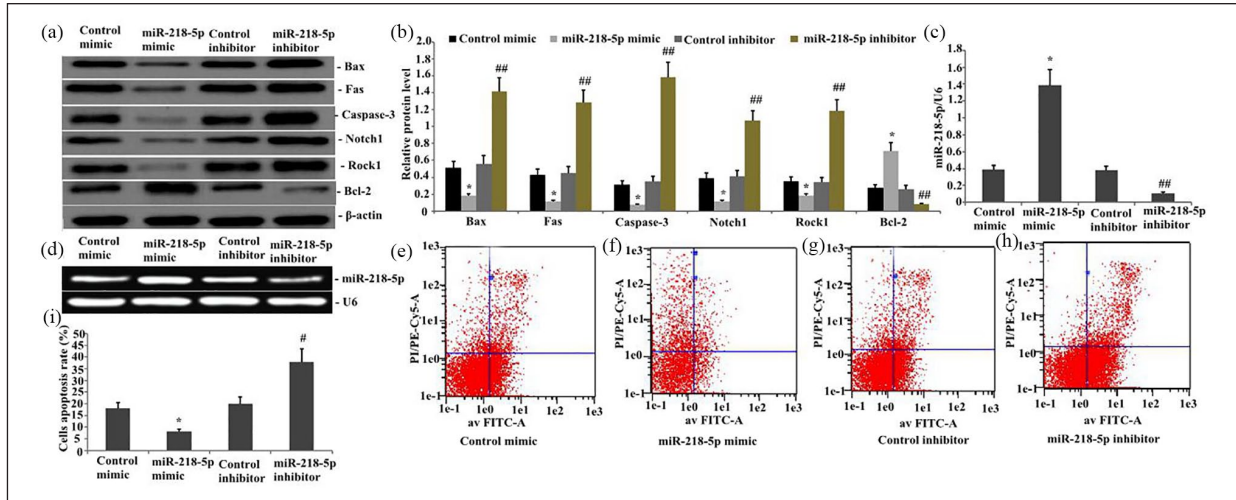
Figure 1. Effect of miR-218-5p on the expression of Bax, Fas, Bcl-2, caspase-3, Rock1, and Notch1 and cell apoptosis in rat intestinal epithelial cells. miR-218-5p mimics, miR-218-5p mimic-negative control (NC), miR-218-5p inhibitor, and miR-218-5p inhibitor-NC were mixed with Lipofectamine 2000 (Invitrogen) and then added to the cell culture. After 24 h of transfection, (a, b) the expression levels of Bax, caspase-3, Fas, Rock1, and Notch1 were measured by Western blot; (c, d) the level of miR-218-5p was measured by RT-PCR; and (e–i) the apoptosis of rat intestinal epithelial cells was measured by flow cytometry. (e) Typical flowchart of rat intestinal epithelial cell apoptosis and (i) the apoptosis rate of rat intestinal epithelial cells by flow cytometry analysis. Data obtained through quantitative densitometry are presented as mean ± SD of three independent experiments. *$P < 0.05$ versus the control group. #$P < 0.05$ versus the model group.
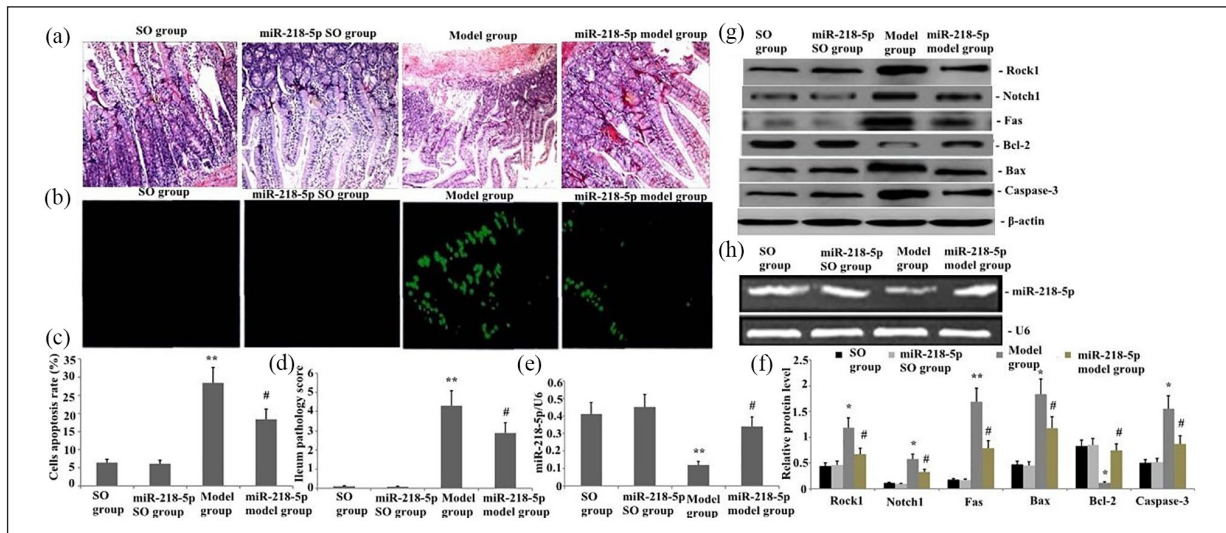
Figure 2. Effect of miR-218-5p overexpression on rat intestinal damage with taurocholate-induced acute pancreatitis. An active miR-218-5p expression construct was delivered to the mice via tail intravenous administration of 1×10^9 pfu of AdCMV-miR-218-5p after 14 days at the time of taurocholate-induced pancreatitis. The rat intestine was histopathologically examined. (a) Representative images of H&E-stained intestinal sections from three experimental groups (magnification, ×400). (b) Representative TUNEL images of the apoptosis of intestinal cells in rats. (c) Percentage of TUNEL-stained intestinal cells in rats. (d) Intestinal damage score. (e, h) Representative RT-PCR and statistical summary of the densitometric analysis showing the level of miR-218-5p in intestines. (f, g) Representative Western blots and statistical summary of the densitometric analysis of the protein expression levels of intestinal Rock1, Notch1, Fas, Bax, Bcl-2, and caspase-3 in rats. Data are represented as mean ± SD of one experiment consisting of three replicates. **$P < 0.01$ versus the control group; ##$P < 0.01$ versus the model group.

increased (Figure 2(e) and (h)). The histopathological examination of the small intestine of taurocholate-treated miR-218-5p rats revealed markedly decreased inflammatory cell infiltration and intestinal damage compared with those of wild-type mice (Figure 2(a) and (d)).
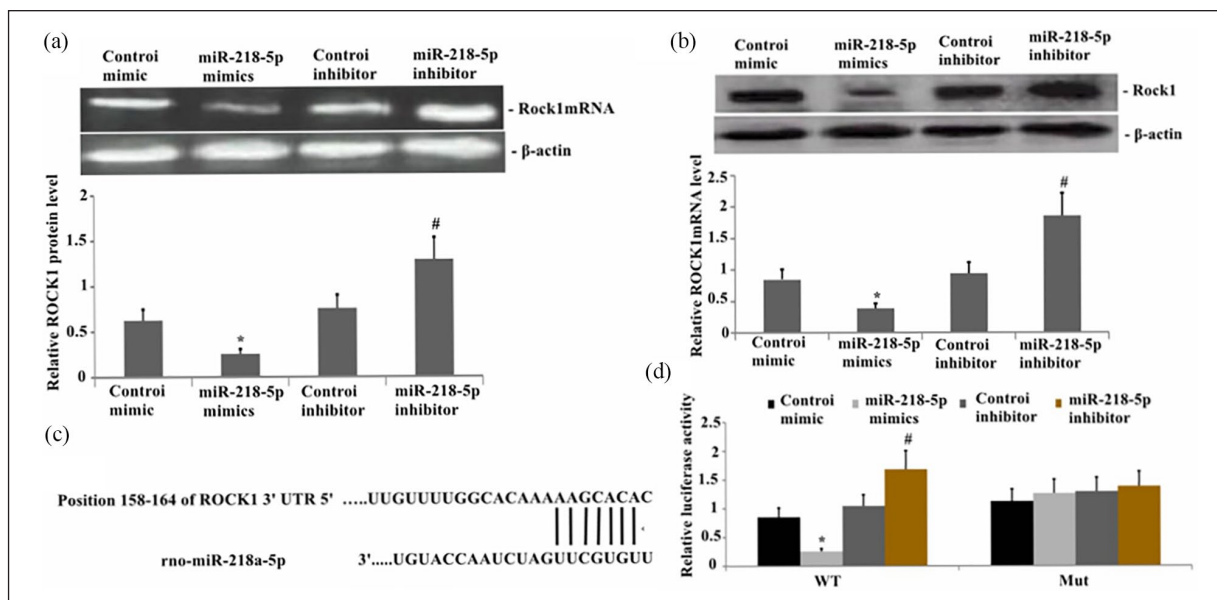
Figure 3. Rock1 is a downstream target of miR-218-5p. (a) Reduced mRNA levels of Rock1 in the rat intestinal epithelial cells after miR-218-5p overexpression ($P < 0.05$). Rock1 expression levels were enhanced after miR-218-5p downregulation ($P < 0.05$). (b) Rock1 decreased in cells with miR-218-5p overexpression compared with that in an empty vector control ($P < 0.05$). Rock1 significantly increased in cells with miR-218-5p downregulation. (c) miR-218-5p bound to the 3′-UTR of Rock1, and binding was interrupted in mutant Rock1. (d) The dual-luciferase reporter assay indicated that the miR-218-5p mimic bound to the 3′-UTR of wild-type Rock1 rather than to Rock1 mutants ($P < 0.05$).

Effect of miR-218-5p overexpression on Rock1, Notch1, Fas, Bax, Bcl-2, and caspase-3 proteins in rat intestinal tissues with taurocholate-induced acute pancreatitis

In this experiment, the increased expression level of miR-218-5p might inhibit the activity of pro-apoptotic proteins and pathways. Rock1, Notch1, Fas, Bax, and caspase-3 proteins were expressed in rats with taurocholate-induced acute pancreatitis to observe the effect of miR-218-5p overexpression on intestinal tissues. The active miR-218-5p expression construct was delivered to rats via the tail intravenous administration of 1×10^9 pfu of AdCMV-miR-218-5p after 14 days at the time when taurocholate was administered to induce pancreatitis. The protein expression levels of Rock1, Notch1, Fas, Bax, and caspase-3 were examined through Western blot analysis; rat intestinal epithelial cell apoptosis was measured by flow cytometry; and miR-218-5p expression was measured through RT-PCR. Figure 2 shows the administration of 1×10^9 pfu of AdCMV-miR-218-5p after 14 days. The expression level of miR-218-5p significantly increased, whereas the protein expression levels of Rock1, Notch1, Fas, Bax, and caspase-3 significantly decreased (Figure 2(g) and (f)), and rat intestinal epithelial cell apoptosis obviously reduced

(Figure 2(b) and (c)) in rat intestinal tissues with taurocholate-induced acute pancreatitis.

Rock1 as a direct miR-218-5p target

Using TargetScan (http://www.targetscan.org), PicTar (www.pictar.org), and miRBase (www.mirbase.org) to predict miRNA targets, we found that Rock1, an important pro-apoptotic regulator of intestinal mucosal injury, was a candidate miR-218-5p target. The mRNA and protein levels of Rock1 were drastically reduced with the overexpression of miR-218-5p (Figure 3(a) and (b)). To further confirm the interaction between Rock1 and miR-218-5p, we constructed Rock1-3′-UTR-wt and Rock1-3′-UTR-mt constructs for dual-luciferase reporter assays (Figure 3(c)). As expected, miR-218-5p bound to Rock1-3′-UTR-wt but not to the mutant type (Figure 3(d)).

Effect of emodin treatment on miR-218-5p expression levels in the intestine after taurocholate-induced acute pancreatitis

In this study, real-time PCR and in situ hybridization assay were performed to determine the expression of miR-218-5p and to observe the effect of emodin treatment on miR-218-5p expression
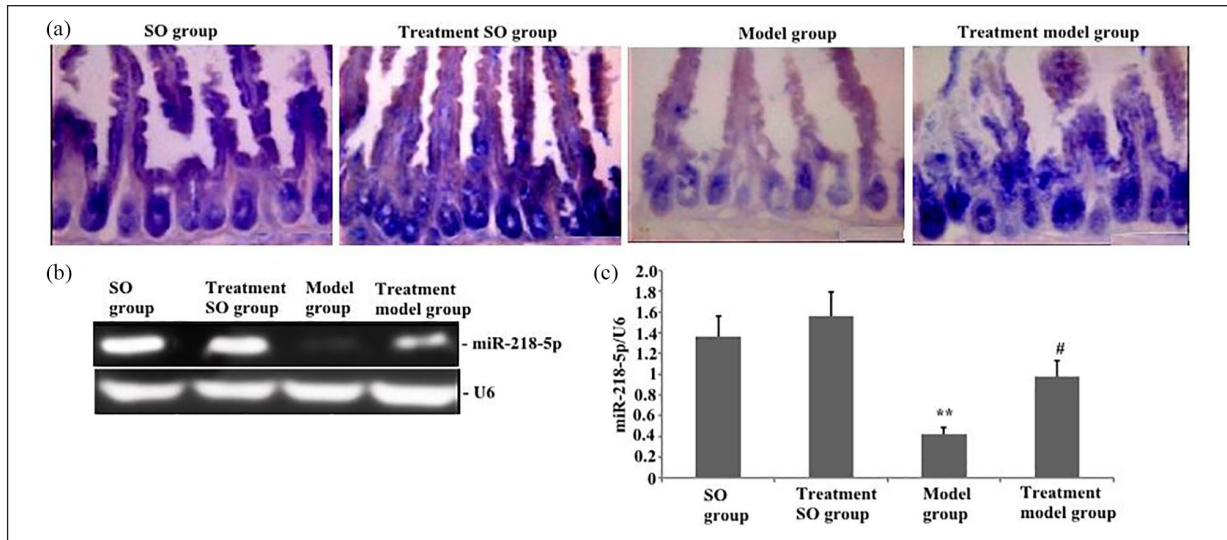
Figure 4. Emodin treatment increased miR-218-5p expression levels in the intestine after taurocholate-induced acute pancreatitis. The rats with SAP were treated with emodin for 24 h. The miR-218-5p expression in the intestine was measured through ISH and RT-PCR. (a) ISH images from the four treatment groups (magnification, ×400). (b, c) Representative RT-PCR and statistical summary of the densitometric analysis of miR-218-5p expression from the four treatment groups. Bars indicate mean ± SD. *$P < 0.05$ and **$P < 0.01$ versus the SO group and treatment SO group; #$P < 0.05$ versus the model group; $P > 0.05$ for the SO mice versus the treatment SO group.

levels in the intestine. In Figure 4, the expression levels of miR-218-5p in SAP-induced intestinal tissues obviously decreased compared with those in the SO group (Figure 4(a)–(c)). However, after emodin therapy was administered, the miR-218-5p expression markedly increased compared with that in the model group (Figure 4(a)–(c)). Therefore, miR-218-5p upregulation by emodin treatment might be involved in the alleviation of intestinal damage with acute necrotizing pancreatitis.

Effect of emodin treatment on gene and protein levels of RhoA, ROCK1, Akt, and Notch1 in the intestine after taurocholate-induced acute pancreatitis

The groups of rats were challenged with taurocholate and treated with emodin 24 h later. RT-PCR and Western blot were conducted to measure the gene and protein expression levels of RhoA, ROCK1, Akt, and Notch1 in intestinal tissues. RT-PCR and Western blot analysis revealed that the gene expression levels of RhoA, ROCK1, Akt, and Notch1 and the protein expression levels of RhoA, ROCK1, p-Akt, and Notch1 were significantly upregulated in intestinal tissues with taurocholate-induced acute pancreatitis (Figure 5(a)–(f)). After emodin therapy was administered,

RhoA, ROCK1, Akt, and Notch1 gene levels and RhoA, ROCK1, p-Akt, and Notch1 protein levels in intestinal tissues significantly decreased (Figure 5(a)–(f)). Therefore, emodin could suppress the expression of RhoA, ROCK1, Akt, and Notch1 (Figure 5(a)–(f)).

Effect of emodin treatment on the expression of apoptotic proteins Bax, Bcl-2, Fas, FasL, caspase-9, and caspase-3 in intestinal tissues of rats with taurocholate-induced acute pancreatitis

To reveal the protective mechanism of emodin treatment by regulating the SAP-induced apoptosis of intestinal mucosal epithelial cells, the intestinal apoptotic protein and gene expression levels of Bax, Bcl-2, Fas, FasL, caspase-9, and caspase-3 were determined 24 h after taurocholate-induced acute pancreatitis. In Figure 6, the protein and gene levels of intestinal Fas, FasL, Bax, caspase-9, and caspase-3 in rats with taurocholate-induced acute pancreatitis significantly increased, whereas the level of Bcl-2 decreased ($P < 0.05$; Figure 6(a)–(d)). Conversely, the levels of intestinal Fas, FasL, Bax, caspase-9, and caspase-3 in rats with taurocholate-induced acute pancreatitis significantly decreased, and the expression of Bcl-2 significantly
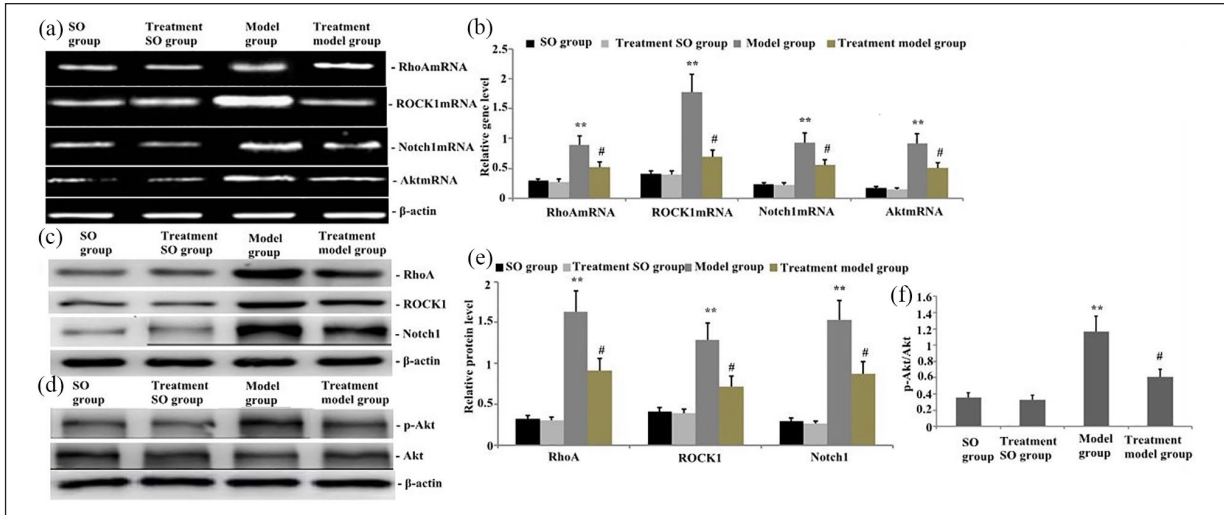
Figure 5. Effect of emodin treatment on RhoA, ROCK1, Akt, p-Akt, and Notch1 gene and protein levels in the intestines after taurocholate-induced acute pancreatitis. (a) Representative RT-PCR showing the gene levels of RhoA, ROCK1, Akt, and Notch1 in the intestine of rats 24 h after emodin was administered. (b) Statistical summary of the densitometric analysis of the gene levels of RhoA, ROCK1, Akt, and Notch1 in the intestine of rats with taurocholate-induced acute pancreatitis. (c, d) Representative Western blots showing the protein expression level of RhoA, ROCK1, p-Akt, and Notch1 in the intestine of rats 24 h after emodin treatment. (e, f) Statistical summary of the densitometric analysis of the protein expression of RhoA, ROCK1, p-Akt, and Notch1 in the intestine of rats with taurocholate-induced acute pancreatitis. Each value represents mean ± SD as determined from three independent experiments. *P < 0.05 and **P < 0.01 versus the SO group and treatment SO group; #P < 0.05 and ##P < 0.01 versus the model group.
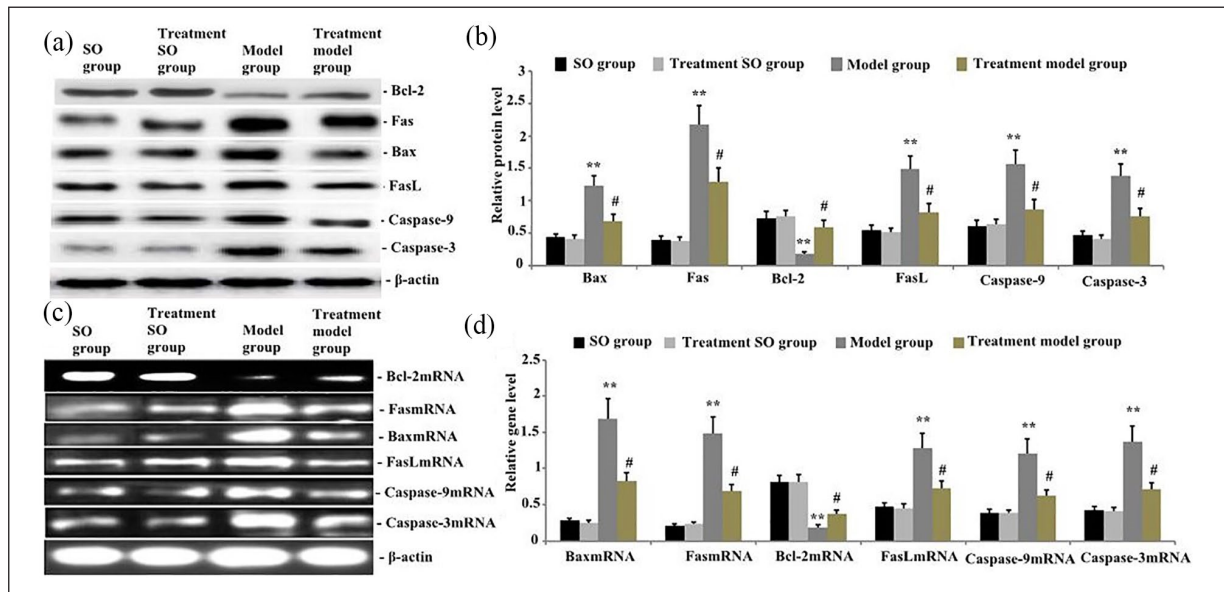
Figure 6. Effect of emodin on the expression of Fas, FasL, Bax, Bcl-2, caspase-9, and caspase-3 in intestinal tissues from rats with taurocholate-induced SAP. The gene and protein expression levels of Fas, FasL, Bax, Bcl-2, caspase-9, and caspase-3 in intestinal tissues from rats with taurocholate-induced SAP were assayed via Western blot and RT-PCR in all of the four treatment groups. (a, b) Representative Western blots and statistical summary of the densitometric analysis showing the protein expression level of Fas, FasL, Bax, Bcl-2, caspase-9, and caspase-3 in the intestine of rats 24 h after emodin treatment. (c, d): Representative RT-PCR and statistical summary of the densitometric analysis showing the gene levels of Fas, FasL, Bax, Bcl-2, caspase-9, and caspase-3 in the intestine of rats 24 h after emodin treatment. Data are represented as mean ± SD of three experiments. *P < 0.05 and **P < 0.01 versus the SO group and treatment SO group; ##P < 0.01 and #P < 0.05 versus the model group.
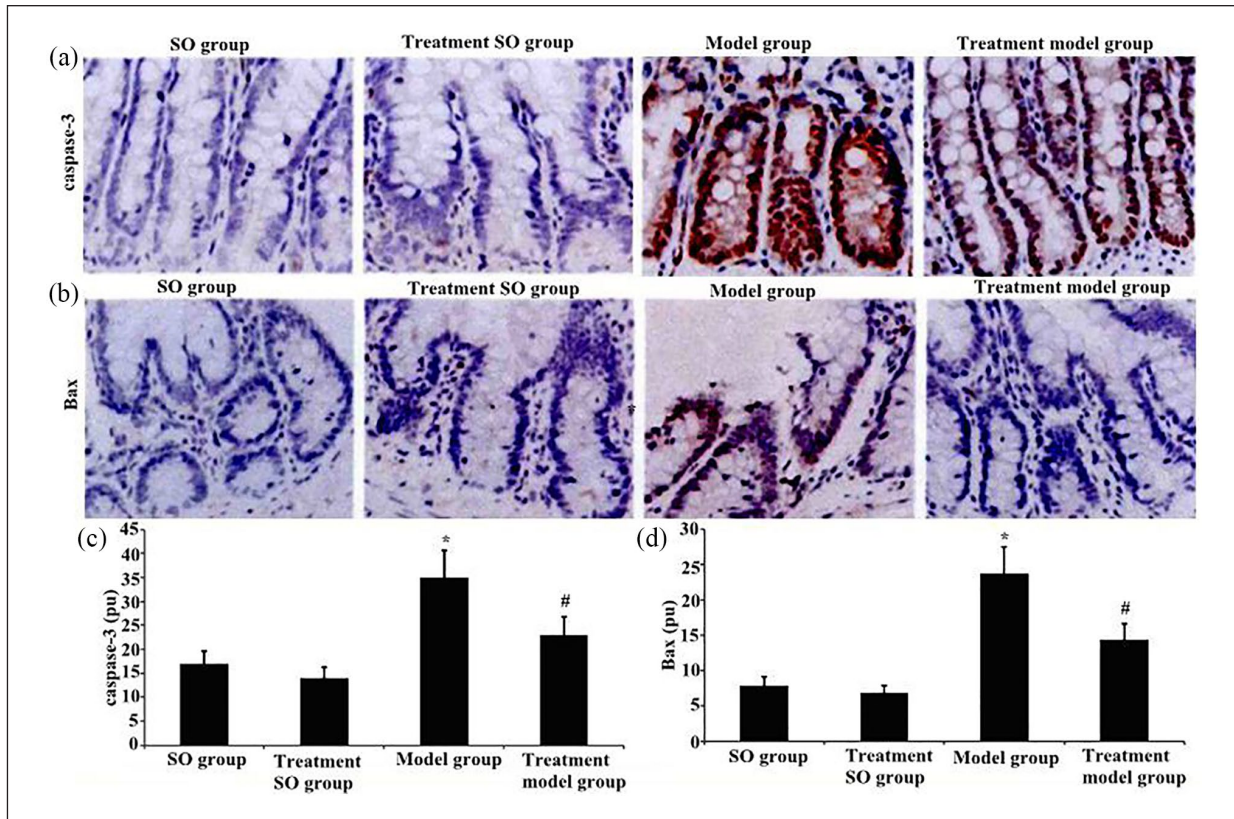
Figure 7. Emodin decreased the positive expression of Bax and caspase-3 in the small intestine of rats with taurocholate-induced SAP. (a, b) Representative immunostaining (brown) patterns of Bax and caspase-3 (magnification, $\times$100). (c, d) Statistical summary of densitometric analyses of Bax and caspase-3 staining. Data are represented as mean $\pm$ SD. *$P < 0.05$ versus the SO group and treatment SO group; #$P < 0.05$ versus the model group.

increased in response to emodin treatment ($P < 0.05$; Figure 6(a)–(d)).

Emodin-induced decrease in the positive expression of Bax and caspase-3 in the small intestine of rats with taurocholate-induced SAP

The rats with taurocholate-induced SAP were treated with emodin for 24 h to investigate the effect of emodin on Bax and caspase-3 activities in the small intestine. The positive expression of Bax and caspase-3 was evaluated via an immunohisto-chemistry assay. In Figure 7, their positive expression in SAP-induced rats significantly increased, but their positive expression significantly decreased in rats treated with emodin compared with those of the model group (Figure 7(a)–(d)). However, no significant difference was observed between the SO group and the treatment SO group ($P > 0.05$). The result showed that emodin could decrease Bax and caspase-3 activities in the small intestine of SAP-induced rats.

Emodin-induced reduction of small intestinal apoptosis after taurocholate-induced acute pancreatitis

To determine the effect of emodin treatment on the apoptosis of intestinal cells from taurocholate-exposed SAP rats, we performed TUNEL (TdT dUTP nick-end labeling) assays. In Figure 8, the apoptotic rate of intestinal cells of rats exposed to taurocholate mark-edly increased compared with that of the SO group. In comparison with the taurocholate group, the group treated with emodin showed a significantly decreased apoptotic rate of intestinal cells (Figure 8(a)–(b)). These data suggested that emodin suppressed the apoptosis of intestinal cells in the SAP rat model.

Effect of emodin treatment on occludin, ZO-1, and claudin-1 protein in rats after taurocholate-induced acute pancreatitis

The disruption of intestinal tight junction postin-jury is determined by gap formation and
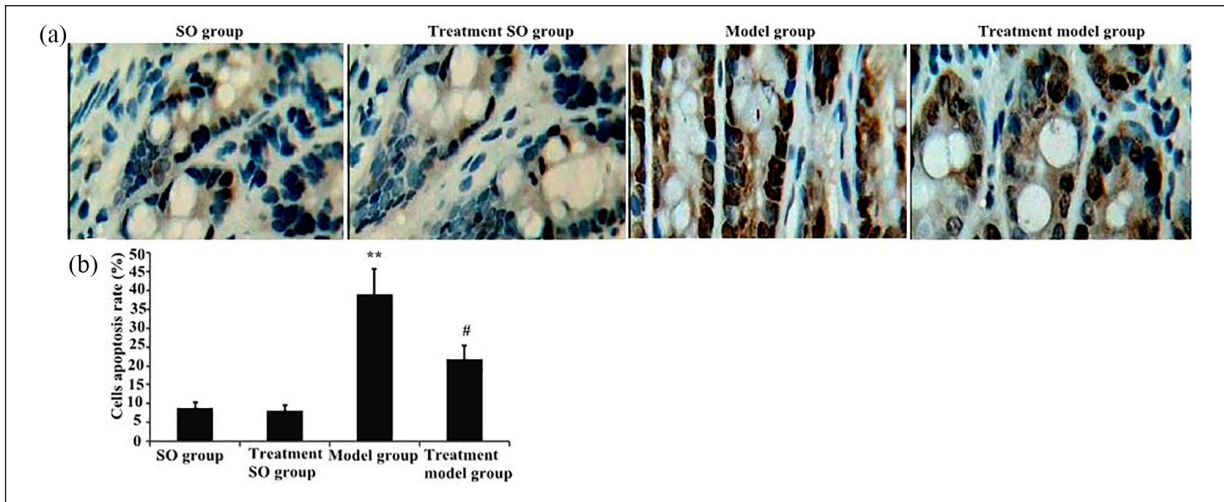
Figure 8. Effect of emodin treatment on the apoptosis of intestinal cells in rats with taurocholate-induced SAP. TUNEL analysis was performed in the four treatment groups. (a) Representative TUNEL images showing the apoptosis of intestinal cells of rats 24 h after emodin administration (magnification, ×200). (b) Intestinal epithelial cell apoptosis rate. Data are represented as mean ± SD. **$P < 0.01$ versus the SO group and treatment SO group; #$P < 0.05$ versus the model group.
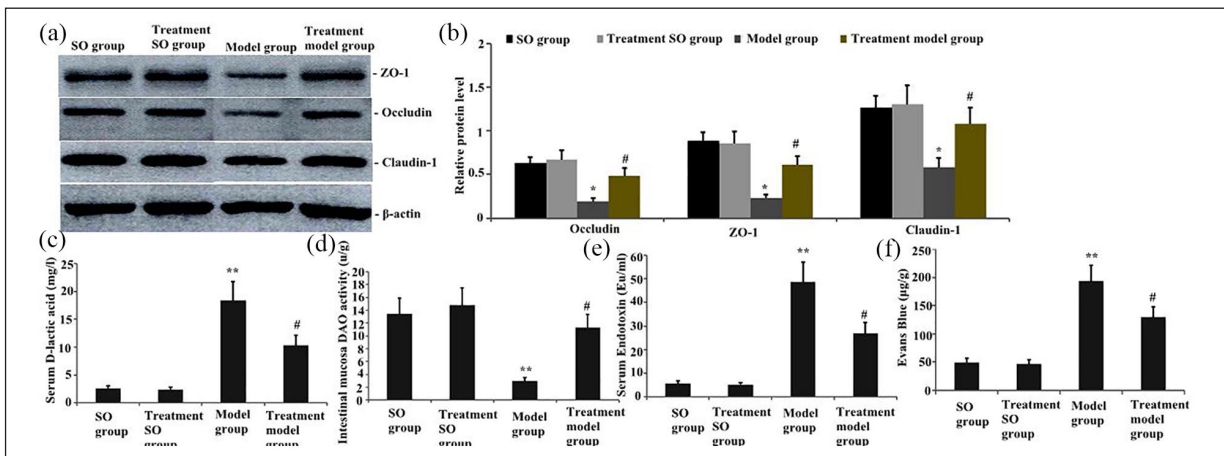
Figure 9. Emodin alleviated the disruption of intestinal tight junction after taurocholate-induced acute pancreatitis. After emodin was administered, (a, b) ZO-1 and claudin-5 protein expression levels were assayed through Western blot in the four treatment groups after taurocholate-induced acute pancreatitis; the serum (c) D-lactic acid, (d) diamine oxidase (DAO), and (e) endotoxin levels were examined through ELISA. (f) Evans blue extravasation assays were performed. Data are expressed as mean ± SD. *$P < 0.05$ and **$P < 0.01$ versus the SO group and treatment SO group; #$P < 0.05$ and ##$P < 0.01$ versus the model group.

rearrangement.[13] To investigate the tight junction rearrangement, we determined intestinal ZO-1, claudin-1, and occludin expression through Western blot analysis. In Figure 9, occludin, ZO-1, and claudin-1 expression levels significantly decreased in the SAP group compared with those in the SO group ($P < 0.05$; Figure 9(a) and (b)). However, the treatment with emodin significantly increased the intestinal occludin, ZO-1, and claudin-1 expression levels after SAP ($P < 0.05$; Figure 9(a) and (b)).

Effect of emodin treatment on serum D-lactic acid and DAO in rats with taurocholate-induced acute pancreatitis

Serum D-lactic acid and diamine oxidase (DAO) are important indicators in the evaluation of intestinal mucosal barrier damage. In this study, serum D-lactic acid and DAO levels were measured through ELISA to explore the role of emodin in acute pancreatitis caused by sodium taurocholate, as shown in Figure 9(c) and (d). After the groups of rats were exposed to
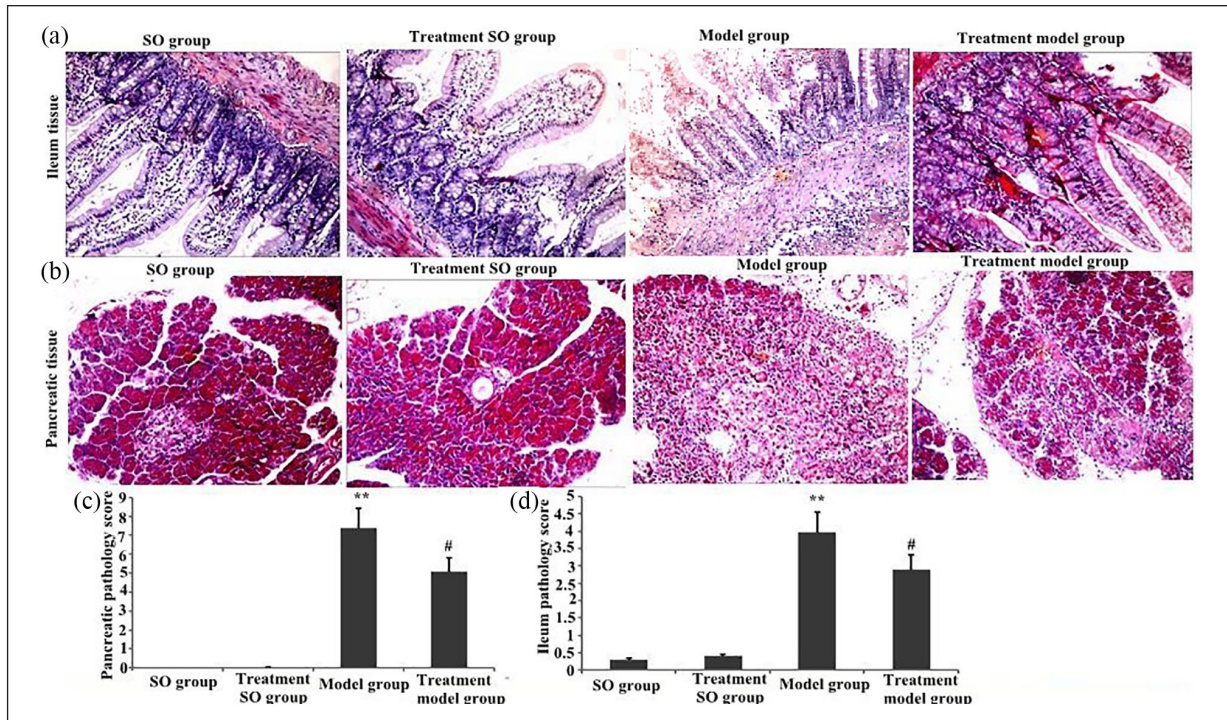
Figure 10. Histopathological changes in small intestinal and pancreatic tissues in rats. (a, b) Histopathological changes in small intestinal and pancreatic tissues from rats (H&E staining, ×100). (c, d) Statistical summary of intestinal and pancreatic pathological scores in rats. Pancreatic and small intestinal injury scores are expressed as mean ± SD from triplicate experiments. **$P < 0.01$ versus the SO group and treatment SO group; ##$P < 0.01$ versus the model group.

taurocholate, serum D-lactic acid and DAO levels were markedly enhanced. In comparison with the taurocholate group, the groups pretreated with emodin markedly decreased the plasma D-lactic acid and DAO levels ($P < 0.05$; Figure 9(c) and (d)).

Emodin suppressed the translocation of intestinal endotoxin after taurocholate-induced acute pancreatitis

The serum endotoxin level in each group was measured to analyze the effect of emodin on intestinal endotoxin translocation after SAP. The results showed that serum endotoxin levels in rats with SAP significantly increased ($P < 0.05$; Figure 9(e)). The endotoxin level after SAP significantly decreased after treatment with emodin was administered ($P < 0.05$; Figure 9(e)).

Emodin-induced decrease in small intestinal epithelial permeability after taurocholate-induced acute pancreatitis

Evans blue extravasation assays were performed to evaluate the effect of emodin on intestinal permeability after SAP. In Figure 9, the dye extravasation

of the SAP group was higher than that of the SO group ($P < 0.05$; Figure 9(f)). However, the treatment with emodin significantly attenuated the leakage of Evans blue caused by SAP ($P < 0.05$; Figure 9(e)).

Emodin-induced alleviation of pancreatic and small intestinal mucosal injury after taurocholate-induced acute pancreatitis

The morphological characteristics of the pancreas and the small intestine were examined and compared with those of the treatment group to assess the effects of emodin on the pancreas and small intestinal mucosal injury after taurocholate-induced acute pancreatitis. The results showed that the SAP group exhibited severe edema and a high degree of histoarchitectural destruction of the acinar cells and the pancreas (Figure 10(a) and (c)). The pathological scores of the small intestine and the pancreas significantly enhanced compared with those in the model group (Figure 10(b) and (d)). By contrast, injury to small intestinal and pancreatic tissues was alleviated in the emodin treatment group, and pancreatic injury scores significantly decreased (Figure 10(a)–(d))

Discussion

The SAP treatment mainly focuses on how to reduce trypsin production and prevent trypsin activation. However, this treatment remains unsatisfactory. Patients with SAP often die from secondary infections and multiple organ dysfunction syndrome.[1] In our experiment, we found large areas with edema, hemorrhage, and inflammatory cell infiltration into the lamina propria in the SAP group. In addition, the ileal mucosa was massively destroyed, and shorter, atrophic, and fractured villi were observed in the SAP group (Figure 10). These changes resulted in a continuous interruption of the intestinal mucosa and impaired the intestinal barrier. To further confirm the effects of SAP on intestinal barrier and permeability, we performed the Evans blue extravasation assay to measure the permeability of the intestinal mucosa. We also measured the intestinal permeability markers, including plasma D-Lactic acid and DAO. SAP-induced intestinal damage exacerbated, and plasma D-lactic acid and DAO levels increased (Figure 9). Intestinal permeability also increased (Figure 9). The distal small intestine and the colon have numerous bacteria; endotoxin, which is released when the cell wall collapses after bacterial cells die, is present in the cell wall of Gram-negative bacteria and can be released by live bacteria through exocytosis.[20] When the intestinal barrier is dysfunctional, the blocking effect on pathogenic microorganisms is reduced, and endotoxin is largely infused into the blood, producing intestinal-derived endotoxemia. Eventually, it can lead to multiple organ dysfunction and exacerbate pancreatic damage.[20] Therefore, plasma endotoxin levels can be used as an objective indicator to assess intestinal mucosal permeability and intestinal barrier function. In our experiment, in the SAP group, intestinal damage aggravated, plasma D-lactic acid and DAO levels significantly increased, intestinal permeability increased, plasma endotoxin levels increased, pancreatic damage aggravated, and the mortality of experimental animals increased. However, after the treatment with emodin, plasma D-lactic acid and DAO levels significantly reduced. Intestinal mucosal permeability, plasma endotoxin levels, and intestinal and pancreatic pathological damage also decreased significantly, and the order of the intestinal mucosal villi was restored compared with that in the SAP group, which showed slight edema and improved integrity of the mucous membranes.

Tight junction (TJ) and adhesion junction (AJ) proteins between epithelial cells are important components of the intestinal mechanical barrier.[21] Among various TJ proteins and AJ proteins, occludin and E-cadherin play the most important roles in the formation and maintenance of the intestinal barrier. Many diseases, such as sepsis and inflammatory bowel disease, can cause dysfunction of the intestinal mucosal epithelial barrier by destroying the normal structure and function of TJ and AJ proteins.[22] In our experiment, when bile sulfonic acid induced severe pancreatitis, the expression of occludin, ZO-1, and E-cadherin in the intestinal tract significantly decreased, intestinal damage aggravated, and intestinal permeability increased (Figure 8). After emodin treatment, the expression levels of occludin, ZO-1, and E-cadherin in the intestinal tract increased significantly; intestinal injury alleviated; intestinal permeability decreased; and the function of the damaged intestinal mucosal epithelial barrier (Figure 8) improved.

Apoptosis plays an important role in the process of intestinal mucosal barrier damage induced by many factors, but the exact mechanism is unknown. Li et al.[23] found that the high expression of miRNA-218-5p can activate two apoptotic pathways, namely, caspase-dependent and non-caspase-dependent pathways, and induce apoptosis in epithelial cell carcinoma. In this experiment, we speculated that microRNA-218-5p may regulate SAP-induced intestinal barrier damage by regulating apoptosis. Our study on rat intestinal epithelial cells revealed that increasing the miRNA-218-5p expression significantly reduced the expression of apoptosis-promoting proteins, such as Fas, FasL, Bax, caspase-9, and caspase-3 proteins (Figure 3), whereas the expression of anti-apoptotic Bcl-2 protein (Figure 3) increased. Flow cytometry showed that the apoptosis of intestinal epithelial cells decreased as the miRNA-218-5p expression increased. Consistently, when the expression of miRNA-218-5p was inhibited, the apoptosis rate of intestinal epithelial cells increased. These results suggested that miR-218-5p might control intestinal mucosal injury induced by bile sulfonic acid by regulating apoptosis. A model of the miRNA-218-5p overexpression was constructed by intravenously injecting ADCMV-miRNA-218-5p with 1×10^9 pfu. Intestinal apoptosis induced by acute

pancreatitis reduced, and mucosal damage also significantly reduced (Figures 3 and 4). These results indicated that increasing the expression of miRNA-218-5p might elicit protective effects by alleviating intestinal barrier injury induced by acute pancreatitis.

After emodin treatment, the miRNA-218-5p expression in the intestinal tissue increased in rats with taurocholate-induced acute pancreatitis (Figure 4). The activity of RhoA/ROCK1 and Notch1 pathway decreased, and the expression levels of apoptosis-related genes and proteins further reduced. Furthermore, the apoptosis rate of intestinal epithelial cells reduced, and the intestinal barrier injury induced by acute pancreatitis improved. Therefore, emodin might inhibit the activity of RhoA/ROCK1 and Notch1 pathways and prevent intestinal barrier damage induced by acute pancreatitis by regulating the expression of miRNA-218-5p. The results showed that the increase in the activity of RhoA/ROCK1 pathways increased epithelial permeability by reorganizing the actin cytoskeleton in pathogenic yeast-induced $CaCO_2$ cells and losing the ZO-1 protein.[24] By contrast, these two phenomena were significantly improved by treating the cells with Fasudil and Y-27632, which are ROCK inhibitors. In this experiment, in acute pancreatitis induced by taurocholate, the expression of RhoA and ROCK1 protein and apoptotic protein increased. By contrast, the expression of occludin, ZO-1, and E-cadherin protein decreased significantly. The epithelial permeability also increased. After emodin administration, the expression of RhoA and ROCK1 protein decreased significantly, and autophagy and apoptotic protein decreased. Conversely, the intestinal occludin, ZO-1, and E-cadherin protein increased significantly, and epithelial permeability improved (Figures 5–8). Acute pancreatitis can activate the Rho/ROCK pathway; promote the autophagy and apoptosis of intestinal epithelial cells; depolymerize F-actin ring; redistribute ZO-1, E-cadherin, and β-catenin proteins in the intestinal tract; and lead to the destruction of intestinal epithelial barrier. After emodin was administered, the activity of the Rho/ROCK pathway decreased; the apoptosis of intestinal epithelial cells reduced; the expression of ZO-1, E-cadherin, and β-catenin protein increased; and the damage to the intestinal epithelial barrier in acute pancreatitis ameliorated.

The NOTCH signaling pathway is closely related to apoptosis.[25] NOTCH can inhibit apoptosis, and the upregulation of NOTCH-1 and NOTCH-4 can inhibit the apoptosis of T-cells and microvascular epithelial cells, respectively.[25] Delta-1, a ligand of NOTCH, can inhibit the apoptosis of mononucleoma cells.[26] Tang et al.[27] found that the downregulation of NOTCH-1 can inhibit the growth of pancreatic cancer cells and induce apoptosis, which may be mediated by regulating the Bcl-2 family. In our experiment, after bile sulfonic acid induced acute pancreatitis, NOTCH-1 expression in the intestinal tissue decreased significantly, Bcl-2 activity decreased, and intestinal epithelial cell apoptosis and autophagy protein increased significantly, causing damage to the intestinal mucosal barrier and increasing the intestinal permeability. On the contrary, after emodin treatment, the NOTCH-1 expression in intestinal tissues increased significantly, and the apoptosis of intestinal epithelial cells and autophagic protein decreased significantly. As a result, the intestinal mucosal barrier improved, and intestinal permeability decreased.

mTOR/Akt is an important apoptosis pathway.[28] Increasing the activity of the NOTCH pathway can inhibit the activity of the mTOR/Akt pathway and promote apoptosis.[29] In our experiment, after bile sulfonic acid induced acute pancreatitis, the activity of the NOTCH pathway increased, the activity of mTOR/Akt was inhibited, and the activities of apoptosis proteins, including Fas, FasL, Bax, caspase-9, and caspase-3, increased in the intestinal tract. Thus, intestinal epithelial apoptosis increased. The protein expression levels of occludin, ZO-1, and E-cadherin were significantly reduced, resulting in an impaired intestinal mucosal barrier and an increase in intestinal permeability. Emodin increased the activities of NOTCH and mTOR/Akt pathways and inhibited the activities of the apoptotic proteins Fas, FasL, Bax, caspase-9, and caspase-3 in the intestine. Emodin also significantly increased the protein expression levels of occludin, ZO-1, and E-cadherin. It also reduced intestinal epithelial apoptosis, resulting in an improved intestinal mucosal barrier and a reduced pancreatic damage.

Previous research found that visnagin improved the antioxidant defense by improving Nrf2 expression, halted pancreatic inflammation by suppressing nuclear factor-κB (NF-κB) and nitrotyrosine expression in the acinar cells, and reduced inflammatory cytokines in lungs and intestine.[30] Berberine

treatment attenuated intestinal barrier injury by inhibiting SAP-induced myosin light chain phosphorylation,[31] and Danshen exerts protective effects on the intestinal mucosa of SAP by inhibiting apoptosis and downregulating NF-κB protein.[32] In this study, emodin reduced intestinal epithelial apoptosis; obviously increased the protein expression levels of occludin, ZO-1, and E-cadherin; improved intestinal mucosal barrier; and reduced pancreatic damage.

Conclusion

Our experiments revealed the underlying mechanism of intestinal mucosal injury induced by SAP and the protective mechanism of emodin against this injury. This experiment demonstrated that miR-218-5p might regulate the activity of RhoA/ROCK and NOTCH signaling pathways to control the intestinal apoptotic pathway and play important roles in alleviating this injury. Our experiment further confirmed that emodin could regulate the expression of miR-218-5p to control RhoA/ROCK and NOTCH signaling pathways; inhibit the activity of apoptosis-related proteins Fas, FasL, Bax, caspase-9, and caspase-3 in the intestine; increase the protein expression of intestinal occludin, ZO-1, and E-cadherin; and reduce the permeability of intestinal mucosa. As a result, the damage to the intestinal mucosal barrier could be reduced, and the intestinal mucosa could be protected from damage caused by acute severe pancreatitis. This study provided a new theoretical basis and therapeutic target for administering rhubarb to treat intestinal mucosal injury induced by SAP.

Limitations of this study

The study illustrated that emodin could block Notch1 and RhoA/ROCK pathways by regulating the expression of miR-218a-5p in the intestine, attenuate intestinal cell apoptosis induced by SAP, and ameliorate the intestinal dysfunction. However, this study had some limitations. In the in vitro study, the effect of different doses of taurocholate on the activity, apoptosis rate, and survival rate of pancreatic acinar cells and intestinal epithelial cells could not be further explored. This experiment failed to investigate the effect of emodin on the activity, survival rate, apoptosis rate, and half of the efficiency of taurocholate-induced pancreatic

acinar cells and intestinal epithelial cells. At the cellular level, this study was unable to reveal the protective mechanism of emodin for intestinal epithelial cells, so further research is needed. At the organism level in vivo, the prognosis, toxicity, side effects, and maximum tolerated dose of emodin in experimental rats could not be examined. The protective effect of emodin on the intestinal tract induced by acute pancreatitis might involve antioxidation, free radical scavenging, anti-inflammation, autophagy, anti-apoptosis, and other processes, but the underlying mechanism should be further explored. The regulatory effect of miR-218a-5p on SAP-induced intestinal mucosal injury might also involve inflammation, apoptosis, autophagy, and oxidative stress, but its molecular mechanism should be further investigated.

ORCID iDs

Ming-wei Liu (iD) https://orcid.org/0000-0002-3728-2350
Chuan-yun Qian (iD) https://orcid.org/0000-0001-5456-6307

References

1. Terao K, Wake H, Adachi N, et al. (2018) Histidine-rich glycoprotein suppresses hyperinflammatory responses of lung in a severe acute pancreatitis mouse model. *Pancreas* 47(9): 1156–1164.
2. Ye C, Wang R, Wang M, et al. (2018) Leptin alleviates intestinal mucosal barrier injury and inflammation in obese mice with acute pancreatitis. *International Journal of Obesity* 42(8): 1471–1479.
3. Xu S, Wei S, Guo Y, et al. (2018) Involvement of nucleotide-binding and oligomerization domain-like receptors in the intestinal injury of severe acute pancreatitis in rats. *Pancreas* 47(2): 245–251.
4. Lu XG, Zhan LB, Liang ZK, et al. (2017) Dai-Huang-Fu-Zi-Tang alleviates pulmonary and intestinal injury with severe acute pancreatitis via regulating aquaporins in rats. *BMC Complementary and Alternative Medicine* 17(1): 288.

5. Sonika U, Goswami P, Thakur B, et al. (2017) Mechanism of increased intestinal permeability in acute pancreatitis: Alteration in tight junction proteins. *Journal of Clinical Gastroenterology* 51(5): 461–466.

6. Lei Q, Qiang F, Chao D, et al. (2014) Amelioration of hypoxia and LPS-induced intestinal epithelial barrier dysfunction by emodin through the suppression of the NF-κB and HIF-1α signaling pathways. *International Journal of Molecular Medicine* 34(6): 1629–1639.

7. Zu C, Qin G, Yang C, et al. (2018) Low dose Emodin induces tumor senescence for boosting breast cancer chemotherapy via silencing NRARP. *Biochemical and Biophysical Research Communications* 505(4): 973–978.

8. Li J, Zhou R, Bie BB, et al. (2018) Emodin and baicalein inhibit sodium taurocholate-induced vacuole formation in pancreatic acinar cells. *World Journal of Gastroenterology* 24(1): 35–45.

9. McKeever PM, Schneider R, Taghdiri F, et al. (2018) MicroRNA expression levels are altered in the cerebrospinal fluid of patients with young-onset alzheimer's disease. *Molecular Neurobiology* 55(12): 8826–8841.

10. Ayeldeen G, Nassar Y, Ahmed H, et al. (2018) Possible use of miRNAs-146a and -499 expression and their polymorphisms as diagnostic markers for rheumatoid arthritis. *Molecular and Cellular Biochemistry* 449(1–2): 145–156.

11. Jauhari A, Singh T and Yadav S (2018) Expression of miR-145 and its target proteins are regulated by miR-29b in differentiated neurons. *Molecular Neurobiology* 55(12): 8978–8990.

12. Yu SF, Feng WY, Chai SQ, et al. (2018). Down-regulation of miR-218-5p promotes apoptosis of human umbilical vein endothelial cells through regulating high-mobility group box-1 in Henoch-Schonlein purpura. *American Journal of the Medical Sciences* 356(1): 64–71.

13. Zhou H, Sun Y, Zhang L, et al. (2018) The RhoA/ROCK pathway mediates high glucose-induced cardiomyocyte apoptosis via oxidative stress, JNK, and p38MAPK pathways. *Diabetes/Metabolism Research and Reviews* 34(6): e3022.

14. Liu MW, Wei R, Su MX, et al. (2018) Effects of Panax notoginseng saponins on severe acute pancreatitis through the regulation of mTOR/Akt and caspase-3 signaling pathway by upregulating miR-181b expression in rats. *BMC Complementary and Alternative Medicine* 18(1): 51.

15. Aho HJ, Koskensalo SM and Nevalainen TJ (1980) Experimental pancreatitis in the rat: Sodium taurocholate-induced acute haemorrhagic pancreatitis. *Scandinavian Journal of Gastroenterology* 15: 411–416.

16. Yu T, Fan Y, Xu Y, et al. (2018) Standardized Ginkgo biloba extract EGb 761® attenuates early brain injury following subarachnoid hemorrhage via suppressing neuronal apoptosis through the activation of Akt signaling. *Biomedicine & Pharmacotherapy* 107: 329–337.

17. Lange S, Delbro DS and Jennische E (1994) Evans blue permeation of intestinal mucosa in the rat. *Scandinavian Journal of Gastroenterology* 29(1): 38–46.

18. Chiu CJ, McArdle AH, Brown R, et al. (1970) Intestinal mucosal lesion in low-flow states: I: A morphological, hemodynamic, and metabolic reappraisal. *Archives of Surgery* 101(4): 478–483.

19. Rongione AJ, Kusske AM, Kwan K, et al. (1997) Interleukin 10 reduces the severity of acute pancreatitis in rats. *Gastroenterology* 112(3): 960–967.

20. Pan LY, Chen YF, Li HC, et al. (2017) Dachengqi decoction attenuates intestinal vascular endothelial injury in severe acute pancreatitis in vitro and in vivo. *Cellular Physiology and Biochemistry* 44(6): 2395–2406.

21. Pan L, Qin G, Zhao Y, et al. (2013) Effects of soybean agglutinin on mechanical barrier function and tight junction protein expression in intestinal epithelial cells from piglets. *International Journal of Molecular Medicine* 14(11): 21689–21704.

22. Jin M, Zhu Y, Shao D, et al. (2017) Effects of polysaccharide from mycelia of Ganoderma lucidum on intestinal barrier functions of rats. *International Journal of Biological Macromolecules* 94(Pt. A): 1–9.

23. Li B, Ding CM, Li YX, et al. (2018) MicroRNA145 inhibits migration and induces apoptosis in human nonsmall cell lung cancer cells through regulation of the EGFR/PI3K/AKT signaling pathway. *Oncology Reports* 40(5): 2944–2954.

24. Banerjee S and McGee DW (2016) ROCK activity affects IL-1-induced signaling possibly through MKK4 and p38 MAPK in Caco-2 cells. *In Vitro Cellular & Developmental Biology: Animal* 52(8): 878–884.

25. Qian W, Lv S, Li J, et al. (2018) Norepinephrine enhances cell viability and invasion, and inhibits apoptosis of pancreatic cancer cells in a Notch1dependent manner. *Oncology Reports* 40(5): 3015–3023.

26. Lu Z, Ren Y, Zhang M, et al. (2018) FLI-06 suppresses proliferation, induces apoptosis and cell cycle arrest by targeting LSD1 and Notch pathway in esophageal squamous cell carcinoma cells. *Biomedicine & Pharmacotherapy* 107: 1370–1376.

27. Tang Y, Tang Y and Cheng YS (2017) miR-34a inhibits pancreatic cancer progression through Snail1-mediated epithelial-mesenchymal transition and the Notch signaling pathway. *Scientific Reports* 7: 38232.

28. Gallardo-Vera F, Tapia-Rodriguez M, Diaz D, et al. (2018) Vanadium pentoxide increased PTEN and decreased SHP1 expression in NK-92MI cells, affecting

PI3K-AKT-mTOR and Ras-MAPK pathways. *Journal of Immunotoxicology* 15(1): 1–11.

29. Zheng J, Li J, Kou B, et al. (2018) MicroRNA-30e protects the heart against ischemia and reperfusion injury through autophagy and the Notch1/Hes1/Akt signaling pathway. *International Journal of Molecular Medicine* 41(6): 3221–3230.

30. Pasari LP, Khurana A, Anchi P, et al. (2019) Visnagin attenuates acute pancreatitis via Nrf2/NFκB pathway and abrogates associated multiple organ dysfunction. *Biomedicine & Pharmacotherapy* 112: 108629.

31. Liang HY, Chen T, Yan HT, et al. (2014) Berberine ameliorates severe acute pancreatitis induced intestinal barrier dysfunction via a myosin light chain phosphorylation dependent pathway. *Molecular Medicine Reports* 9(5): 1827–1833.

32. Zhang XP, Jiang J, Yu YP, et al. (2010) Effect of Danshen on apoptosis and NF-κB protein expression of the intestinal mucosa of rats with severe acute pancreatitis or obstructive jaundice. *Hepatobiliary & Pancreatic Diseases International* 9(5): 537–546.